Influenza A virus nucleoprotein selectively decreases neuraminidase gene-segment packaging while enhancing viral fitness and transmissibility

Christopher B. Brooke[1], William L. Ince[1], Jiajie Wei, Jack R. Bennink, and Jonathan W. Yewdell[2]

Laboratory of Viral Diseases, National Institute of Allergy and Infectious Diseases, National Institutes of Health, Bethesda, MD 20892

Edited by Robert A. Lamb, Northwestern University, Evanston, IL, and approved October 17, 2014 (received for review August 10, 2014)

The influenza A virus (IAV) genome is divided into eight distinct RNA segments believed to be copackaged into virions with nearly perfect efficiency. Here, we describe a mutation in IAV nucleoprotein (NP) that enhances replication and transmission in guinea pigs while selectively reducing neuraminidase (NA) gene segment packaging into virions. We show that incomplete IAV particles lacking gene segments contribute to the propagation of the viral population through multiplicity reactivation under conditions of widespread coinfection, which we demonstrate commonly occurs in the upper respiratory tract of guinea pigs. NP also dramatically altered the functional balance of the viral glycoproteins on particles by selectively decreasing NA expression. Our findings reveal novel functions for NP in selective control of IAV gene packaging and balancing glycoprotein expression and suggest a role for incomplete gene packaging during host adaptation and transmission.

influenza virus | genome segmentation | genome packaging | nucleoprotein | host adaptation

Seasonal influenza A virus (IAV) remains a major public health threat, causing tens of thousands of deaths each year in the United States alone (1). Morbidity and mortality rates can increase dramatically when a zoonotic strain adapts to circulate in humans, triggering a pandemic. The continuing toll exerted by IAV stems from its remarkable adaptability, which enables it to move between widely divergent host species and also evade herd immunity within each species. Defining the specific mechanisms that mediate IAV adaptation is essential to improving anti-IAV vaccines, therapeutics, and pandemic surveillance.

The IAV genome consists of eight negative-sense RNA segments, each of which is required for productive infection. Genome segmentation complements the high mutation rate of IAV by facilitating reassortment, which can maximize positive intergenic epistasis (2–5) and allow selective elimination of segments with deleterious mutations (6, 7). Although reassortment is the most obvious and best-characterized benefit of segmentation, there are likely additional evolutionary advantages.

Genome segmentation imposes the substantial constraint of maintaining a gene-packaging mechanism to produce fully infectious virions (8). For IAV, it is widely believed that a single copy of each segment is packaged into progeny virions with nearly perfect efficiency, resulting in an equimolar ratio of the segments at the population level (9–12). Confounding this model, we recently demonstrated that most IAV virions fail to express one or more gene products (13). This finding raises the possibility that in some circumstances incomplete influenza gene packaging is evolutionarily neutral and possibly even advantageous (14).

The viral glycoproteins HA and neuraminidase (NA) are encoded by separate genome segments. HA attaches IAV to terminal sialic acid residues on the host cell surface, enabling viral entry. By hydrolyzing sialic acids, NA detaches budding virions and neutralizes HA-inhibiting glycoproteins and is required for the spread of IAV within and between hosts (15–18). Because the specificity of HA and NA for different sialic acid linkages and contexts can vary substantially, functional alignment between the yin–yang activities of HA and NA represents a major determinant of host adaptation, transmissibility, and immune escape (19–23). Independently controlling levels of HA and NA expression therefore may be critical for fine-tuning their functional balance.

We previously described a single amino acid substitution (F346S) in the nucleoprotein (NP) of mouse-adapted A/Puerto Rico/8/34 (PR8), selected during serial passage in guinea pigs, which enhances replication in the guinea pig respiratory tract and enables contact transmission (4). Here, we report that this adaptive mutation selectively decreases both the expression and packaging of the NA gene segment, thus revealing a surprising role for NP in the regulation of glycoprotein function and demonstrating that decreased gene packaging can be associated with increased in vivo fitness and transmissibility.

Results

NP Selectively Regulates NA Expression and Glycoprotein Functional Balance. While characterizing the NP:F346S mutation, we observed by immunoblotting that purified $PR8_{NP:F346S}$ virions (generated by reverse genetics to ensure a genetic background similar to wild-type virus stocks) contained 10-fold less NA than wild-type virus ($PR8_{WT}$), as normalized either to absolute virion numbers (based on hemagglutination units; HAU) or to HA or matrix (M1) levels (Fig. 1*A*). Concomitantly, purified $PR8_{NP:F346S}$ virus exhibited a similar decrease in NA enzymatic activity per particle, as determined by HAU, revealing an unexpected role for NP in modulating virion NA content (Fig. 1*B*).

Does the decrease in NA virion incorporation stem from decreased cellular expression of NA? We infected Madin–Darby

Significance

The influenza A virus (IAV) genome consists of eight unique RNA segments, each of which is required for productive infection. IAV is believed to copackage its individual gene segments into virions with nearly perfect efficiency to maximize replicative potential. We contradict this view by demonstrating that decreased gene packaging can be associated with increased in vivo fitness and transmissibility. Incomplete packaging likely is facilitated by the extensive coinfection that we demonstrate in vivo, which promotes complementation and explains the frequent reassortment reported previously. We also reveal roles for the viral nucleoprotein in modulating glycoprotein function and gene packaging during host adaptation. These findings necessitate a major shift in how we think about the infectious and evolutionary potential of IAV populations.

Author contributions: C.B.B., W.L.I., J.R.B., and J.W.Y. designed research; C.B.B., W.L.I., and J.W. performed research; C.B.B., W.L.I., J.R.B., and J.W.Y. analyzed data; and C.B.B., W.L.I., J.R.B., and J.W.Y. wrote the paper.

The authors declare no conflict of interest.

This article is a PNAS Direct Submission.

[1]C.B.B. and W.L.I. contributed equally to this work.

[2]To whom correspondence should be addressed. Email: jyewdell@niaid.nih.gov.

This article contains supporting information online at www.pnas.org/lookup/suppl/doi:10.1073/pnas.1415396111/-/DCSupplemental.

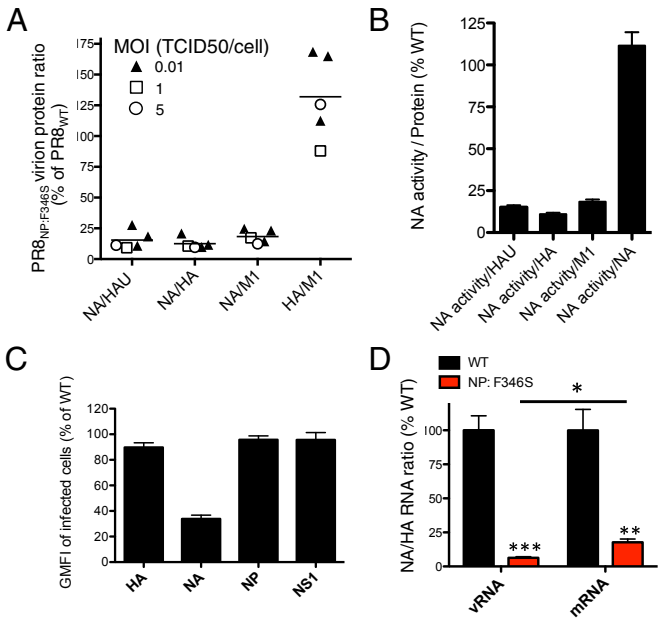

Fig. 1. NP modulates virion glycoprotein balance through epistatic control of NA expression. (*A*) Relative protein content of HA, NA, and M1 in purified particle preparations. $P < 0.0001$ for differences between all NA ratios for $PR8_{WT}$ and $PR8_{NP:F346S}$ (one-way ANOVA, Tukey test). Each data point represents a comparison of independent stocks of $PR8_{WT}$ and $PR8_{NP:F346S}$ grown at the indicated MOIs. (*B*) NA activity for purified $PR8_{NP:F346S}$ normalized to average HAU or HA or M1 protein as a percentage of the $PR8_{WT}$ control, presented as mean ± SEM; $P < 0.0001$ for differences between all NA ratios compared with the matched wild-type control (one-way ANOVA, Tukey test). (*C*) Relative viral protein expression as determined by geometric mean fluorescence intensity (GMFI) on MDCK cells infected at an MOI <0.05 with $PR8_{WT}$ or $PR8_{NP:F346S}$ that stained positive for the indicated viral proteins. $PR8_{NP:F346S}$ values are presented as the mean percentage of $PR8_{WT}$ ± SEM of three technical replicates. (*D*) Relative copy numbers of HA and NA vRNA and mRNA in FACS-sorted, singly infected HA^+NA^+ cells presented as mean ± SEM, as determined by strand-specific quantitative real-time RT-PCR (*$P < 0.05$; **$P < 0.01$; ***$P < 0.001$; *t* test).

canine kidney (MDCK) cells at a multiplicity of infection (MOI) of <0.05 with $PR8_{WT}$ or $PR8_{NP:F346S}$ to ensure that cells received no more than a single particle, thus normalizing the number of input NA gene segments to one per NA-expressing cell. Under these conditions, $PR8_{NP:F346S}$-infected cells expressed threefold less NA than did $PR8_{WT}$-infected cells, as measured by flow cytometry, whereas HA, NP, and nonstructural protein 1 (NS1) expression levels remained similar (Fig. 1*C*). NA expression also was reduced selectively in cells infected at high MOI (Fig. S1).

To determine whether decreased NA expression is caused by diminished NA RNA, we infected MDCK cells at low MOI and sorted live HA^+NA^+ cells at 7 hours postinfection (hpi). This approach served to normalize the input of HA and NA gene segments to one per examined cell. Quantitative RT-PCR on sorted cells revealed that NP:F346S dramatically reduced the intracellular abundance of both NA viral RNA (vRNA) and mRNA relative to HA RNA (Fig. 1*D*). We next used a virus-free system in which plasmid-encoded wild-type and mutant RNPs were provided with NA vRNA in excess from a human RNA polymerase I-driven expression plasmid to assess the impact of NP:F346S on NA expression when vRNA is not limiting. Under these conditions, NA expression was unaffected by NP:F346S, suggesting that the observed reduction in NA mRNA in the sorted cells is likely a secondary effect of the reduction in NA vRNA (Fig. S2). Thus, NP:F346S likely reduces NA expression by selectively reducing intracellular NA vRNA abundance.

Reducing NA Activity Alone Does Not Enhance Fitness in Guinea Pigs. We next examined the phenotype of NP:F346S in vivo, in the context of a guinea pig-adapted PR8 variant virus, which has a single amino acid substitution in M1 (V166M). M1:V166M allows PR8 to replicate to high titer in guinea pigs, with or without NP:F346S (4), but alone has no detectable effect on selective viral gene expression (Fig. S3). We used the M1:V166M background to eliminate the large differences in replication kinetics between $PR8_{WT}$ and $PR8_{NP:F346S}$ in guinea pigs and to allow a more direct assessment of the effect of NP:F346S in vivo.

We inoculated guinea pigs intranasally (i.n.) with a 10^3 50% tissue culture infective dose ($TCID_{50}$) of $PR8_{M1:V166M}$ or $PR8_{NP:F346S+M1:V166M}$ and collected nasal wash fluids and nasal turbinate cells at 48 hpi, near peak shedding. Importantly, both flow cytometric analysis of viral gene expression in infected nasal turbinate cells and quantitation of viral proteins in nasal wash demonstrated that NP:F346S selectively reduced NA expression in vivo (Fig. 2 *A*–*C*).

To examine the relationship between NA activity and enhanced fitness of $PR8_{NP:F346S}$, we assessed the effects of two independent *cis*-acting NA substitutions (NA:K239R or NA:G339S, numbering from first ATG) that reduce virion NA content by approximately fivefold on viral replication of PR8 in guinea pigs (Fig. S4) (22, 23). Each mutation diminished PR8 replication, indicating that reducing NA expression/activity alone is insufficient to enhance PR8 replication in guinea pigs (Fig. 2*D*).

NP:F346S Selectively Reduces NA Gene-Segment Packaging. We previously reported that the majority of virions in IAV preparations fail to express one or more viral gene products (13). Low-MOI infection revealed that the fraction of $PR8_{NP:F346S}$ virions that express detectable levels of NA upon infection was reduced by approximately threefold relative to $PR8_{WT}$, whereas the frequencies of HA, NP, and NS1 expression were essentially unchanged (Fig. 3 *A* and *B*).

To determine whether this decrease reflects a reduction in NA gene-segment packaging, we performed segment-specific quantitative RT-PCR on purified particles using primers targeting the flanking regions containing the gene-segment packaging signals (8). $PR8_{NP:F346S}$ populations contained threefold fewer NA vRNA copies relative to M1 and HA, compared with $PR8_{WT}$ (Fig. 3*C*). Importantly, vRNA extracted from guinea pig nasal wash collected at peak shedding exhibited a similar selective relative decrease in NA segment vRNA (Fig. 3*D*).

These results clearly establish that NP:F346S reduces relative NA gene packaging in vitro and in vivo, potentially by reducing intracellular NA vRNA abundance.

$PR8_{NP:F346S}$ Produces More Semi-Infectious Particles per Infected Cell. The selective reduction in NA vRNA packaging by NP:F346S should increase the fraction of propagation-deficient semi-infectious (SI) particles relative to fully infectious (FI) virions, because of the lack of an NA segment (13). Indeed, when we infected cells with equivalent tissue culture infectious doses ($TCID_{50}$, a measure of FI virions), $PR8_{NP:F346S}$ infected up to eightfold more cells than $PR8_{WT}$, as measured by cellular NP expression (a measure of both FI and SI virions) (Fig. 3*E*). This effect was confirmed when we compared the ratios of physical particles (determined by HAU) to $TCID_{50}$ (Fig. S5).

A decrease in relative NA gene-segment packaging could result in a decrease in FI particle production, an increase in SI particle production, or a combination of both. Thus, we determined the effect of NP:F346S on the number of FI and SI particles produced during a single infection cycle. We infected MDCK cells with $PR8_{WT}$ or $PR8_{NP:F346S}$ at an MOI of 0.01 ($TCID_{50}$ per cell), collected supernatants between 8 and 9 hpi, and determined the number of FI (measured by $TCID_{50}$) and SI (measured by single-round flow cytometric infection assay) particles. At the time of harvest, we collected the producer cell monolayer and determined the number of $HA^+NP^+NA^+NS1^+$ cells by flow cytometry, which served as a surrogate for productively infected cells. From this

MICROBIOLOGY

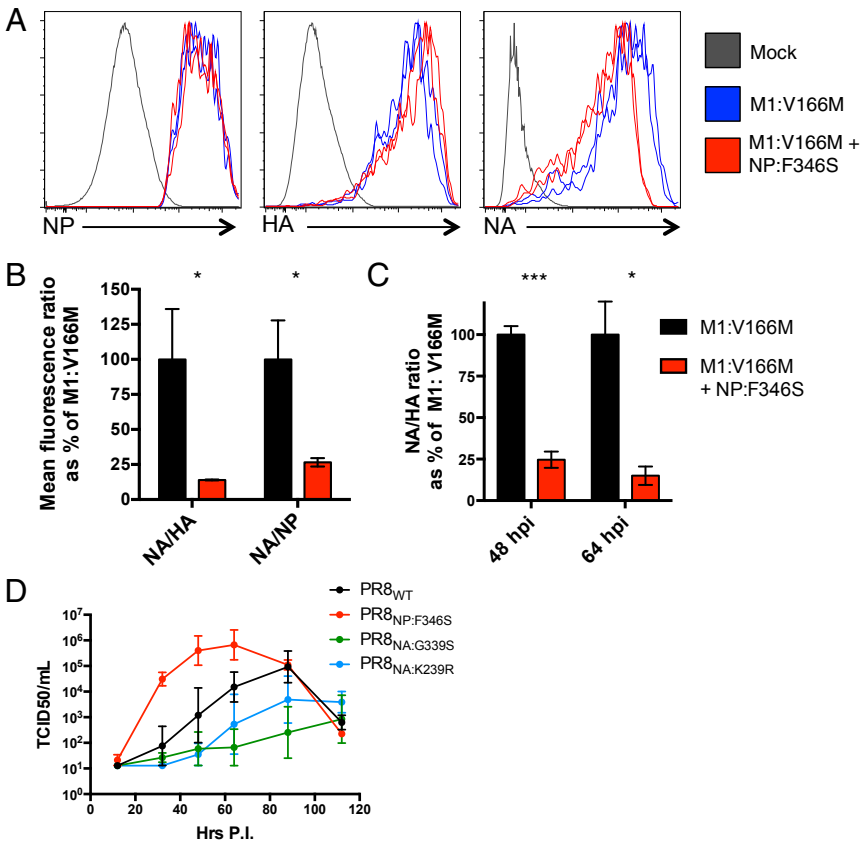

Fig. 2. NP controls NA expression in vivo. (*A* and *B*) Viral protein expression in nasal turbinate cells collected from guinea pigs ($n = 2$) 48 h after i.n. infection with 10^3 $TCID_{50}$ of $PR8_{M1:V166M}$ or $PR8_{M1:V166M+NP:F346S}$ viruses as determined by flow cytometry. (*A*) Comparison of NP, HA, and NA expression within $NP^+HA^+NA^+$ cells. (*B*) The mean per-cell fluorescence ratios for the indicated stains were calculated for $NP^+HA^+NA^+$ cells. Data represent the mean ± SEM (*$P < 0.05$; *t* test). (*C*) Ratio of NA activity (determined using MUNANA substrate) and HA content measured by ELISA in nasal wash from animals ($n = 3$) infected with 10^3 $TCID_{50}$ of $PR8_{M1:V166M}$ or $PR8_{M1:V166M+NP:F346S}$ viruses. Data are presented as mean ± SEM (***$P < 0.001$ *$P < 0.05$; *t* test). (*D*) Nasal wash titers from guinea pigs infected i.n. with 500 $TCID_{50}$ of the indicated viruses ($n = 3$). Data are presented as mean ± SEM.

result we could calculate the average number of FI and SI particles produced per productively infected cell. We detected a slight decrease in the number of FI particles released from productively infected cells by $PR8_{NP:F346S}$ as compared with $PR8_{WT}$ across multiple independent experiments ($P = 0.09$). Concomitantly, we detected a more significant ($P = 0.04$) increase in the number of SI particles produced by the mutant (Fig. 4*A*). This result indicates that $PR8_{NP:F346S}$ produces more SI particles per cycle of replication, perhaps at the partial expense of FI particles.

SI Particles Contribute to Replication Through Multiplicity Reactivation. How can decreased NA vRNA packaging and increased SI particle production be associated with increased in vivo replication kinetics? We hypothesized that the increased number of SI particles produced by $PR8_{NP:F346S}$ contributes to productive replication through multiplicity reactivation, a phenomenon in which coinfecting complementary incomplete particles generate a productive infection (24, 25). If this hypothesis is correct, increasing the MOI should have a more pronounced effect on the virus output of $PR8_{NP:F346S}$ than of $PR8_{WT}$, because the mutant population has a larger fraction of SI particles relative to FI particles.

To test this notion, we compared single-cycle infectious virus output in MDCK cells infected with $PR8_{WT}$ or $PR8_{NP:F346S}$ over a range of input MOIs (based on $TCID_{50}$). FI virion output was indistinguishable between the viruses at an MOI of 0.01, but increasing the MOI significantly increased the infectious virus output of $PR8_{NP:F346S}$ compared with that of $PR8_{WT}$ (Fig. 4*B*).

These results demonstrate that the SI particles produced in greater numbers by $PR8_{NP:F346S}$ than by $PR8_{WT}$ can contribute to the propagation and expansion of the viral population through complementation and multiplicity reactivation under conditions of frequent coinfection.

Coinfection Is Common in Vivo. The importance of multiplicity reactivation during natural infection depends entirely on the prevalence of coinfection in vivo. Although the high frequency of reassortants generated during guinea pig infection demonstrates that coinfection occurs in vivo (4, 26, 27), its actual incidence is unknown.

To determine the coinfection frequency in vivo, we exploited the observation that the cellular coexpression frequencies of specific viral gene products predictably increase with MOI because of complementation (Fig. 5). We infected guinea pigs i.n. with $PR8_{M1:V166M}$, with or without the NP:F346S substitution, and collected nasal wash and turbinates at 9 and 48 hpi. We infected MDCK cells at an MOI ≤0.05 $TCID_{50}$ with virus obtained from the nasal wash at 48 hpi to establish the HA/NA coexpression frequencies for in vivo-produced virus under low-MOI conditions. We then compared these values with the HA/NA coexpression frequencies in NP^+ cells isolated from the nasal turbinates of the same animals (Fig. 6 *A* and *B*).

Nasal turbinate cells collected at 9 hpi exhibited low viral protein coexpression frequencies, demonstrating that (*i*) the initial round of infection occurs under low-MOI conditions following direct inoculation, and (*ii*) the incomplete expression patterns observed in MDCK cells infected at low MOI recapitulate what is seen in vivo. Importantly, by 48 h after infection with 10^3 $TCID_{50}$, each virus attained coexpression frequencies of ∼80–90%, much higher than

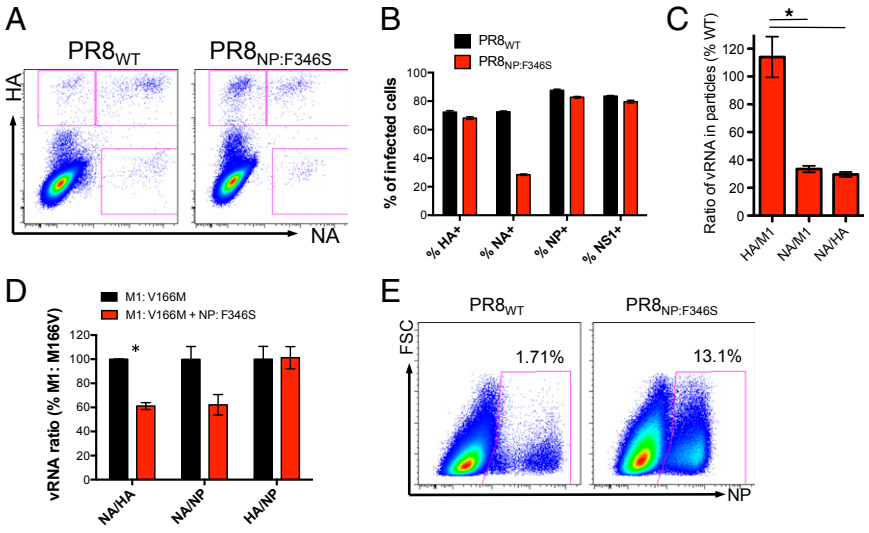

Fig. 3. NP selectively reduces relative NA gene-segment packaging. (*A*) Representative flow cytometry plots of viral protein expression in cells infected at an MOI <0.05 with equal HAEU. (*B*) The population expression pattern illustrated as the percentage of cells in *A* that expressed detectable levels of the indicated proteins. Data represent mean ± SEM of three technical replicates. (*C*) Relative HA, NA, and M vRNA content in purified $PR8_{NP:F346S}$ virus preparations determined by quantitative RT-PCR as a percentage of the matched $PR8_{WT}$ controls. Data are presented as mean ± SEM (*$P < 0.05$; *t* test). (*D*) Relative abundance of vRNA segments as determined by quantitative PCR in nasal wash of $PR8_{M1:V166M+NP:F346S}$-infected guinea pigs ($n = 2$) 48 hpi as a percent of values from $PR8_{M1:V166M}$-infected guinea pigs. Data are presented as mean ± SEM (*$P < 0.05$; *t* test). (*E*) NP expression in MDCK cells infected at an MOI of 0.01 $TCID_{50}$ per cell with $PR8_{WT}$ or $PR8_{NP:F346S}$.

the 40–60% observed during low-MOI ex vivo infection with nasal wash virus and indicative of frequent coinfection.

Together, our results demonstrate that widespread coinfection, and thus the conditions necessary for efficient multiplicity reactivation of SI particles, occurs in guinea pigs by the time of peak shedding. Further, they provide an explanation for how SI particles can contribute to viral replication, thus minimizing the detrimental effects that might be expected from a decrease in gene-packaging efficiency.

Changes in Population-Level Gene-Segment Abundance Directly Influence Viral Gene Expression in Cells. Under high-MOI conditions, such as occur in guinea pigs by 48 hpi, cells infected with $PR8_{NP:F346S}$ will receive on average fewer copies of the NA gene segment than of the other gene segments. This disparity results in a divergence in the effective MOIs of the individual gene segments. Because the kinetics of IAV gene expression increase with MOI, this divergence should generate a gene-dosage effect that reduces NA expression relative to other gene products (28). To test this notion, we generated a stock of PR8 lacking the NA vRNA segment ($PR8_{NoNA}$) using reverse genetics. $PR8_{NoNA}$, although incapable of NA expression, retained HA, NP, and NS1 expression in infected cells (Fig. S6).

We coinfected Vero cells with $PR8_{WT}$ along with increasing doses of $PR8_{NoNA}$ to mimic the altered NA gene-segment frequency in the $PR8_{NP:F346S}$ virus population and assessed relative NA expression within the HA^+NA^+ population by flow cytometry at 15 hpi (Fig. 6*C*). We observed a dose-dependent decrease in NA expression relative to HA. Ratios of NP and NS1 to HA remained relatively constant, indicating that we were not observing a general effect from increasing input virus. At the 1:2 ratio of wild-type to $PR8_{NoNA}$, which best approximates the gene-segment frequencies of $PR8_{NP:F346S}$, we observed a twofold decrease in relative NA expression.

These results demonstrate that the relative abundance of the individual gene segments in an IAV population can directly govern viral gene expression in multiply infected cells.

Discussion

Our findings reveal an unappreciated role for genome segmentation in precisely regulating the packaging and expression of individual viral genes through intergenic epistatic interactions. Segment-specific regulation is particularly important for the HA and NA genes, because balancing the relative activity levels of these two molecules is key to maintaining optimal fitness across different host contexts (20, 21, 29). Previously described mechanisms of NA regulation in response to selective pressure entail *cis*-acting mutations that modulate NA activity in cells or virions (22, 30–32). NA activity on virions also can be influenced *in trans* by M1 and the viral polymerase proteins PB2 and PB1, although the specific mechanisms involved are uncertain (33, 34).

Our discovery that NP can regulate HA/NA functional balance through selective control of NA gene expression reveals yet another mechanism for modulating this critical viral parameter. Identifying the unique properties of the NA gene that enable its selective regulation is the focus of ongoing studies. Deeper

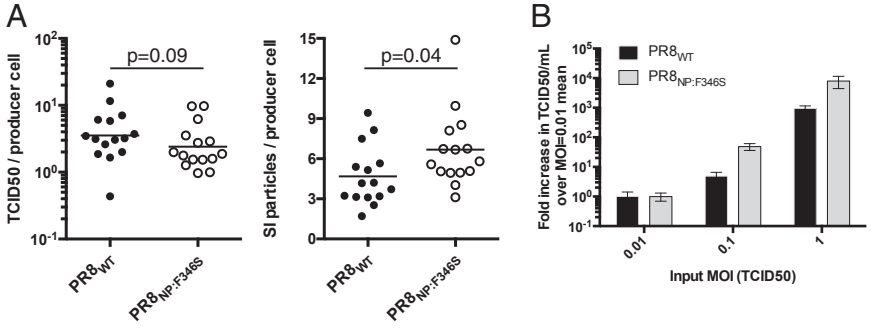

Fig. 4. SI particles contribute to replication through multiplicity reactivation. (*A*) Mean $TCID_{50}$ and SI particle output per $HA^+NP^+NA^+NS1^+$ producer cell by 8–9 hpi. Data are pooled from two independent experiments, and each point represents the value obtained from a single culture. $P = 0.0885$ for $TCID_{50}$; $P = 0.0406$ for SI particles; Mann–Whitney test. (*B*) Virus output (in $TCID_{50}$/mL) from MDCK cells infected for 8 h with $PR8_{WT}$ or $PR8_{NP:F346S}$ presented as the fold increase over output at an MOI of 0.01 for three stocks grown in parallel at each MOI ± SEM. Interaction between strain and MOI: $P = 0.0308$ by two-way ANOVA.

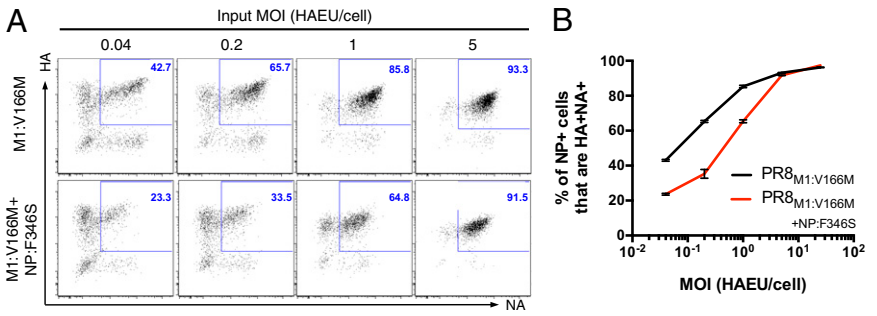

Fig. 5. The frequency of viral protein coexpression increases with MOI. MDCK cells were infected for 9 h with $PR8_{M1:V166M}$ or $PR8_{M1:V166M+NP:F346S}$ at the indicated MOIs, and the percentage of NP^+ cells that also express HA and NA was determined by flow cytometry. (*A*) Representative dot plots. (*B*) Mean ± SEM of two replicates per condition.

understanding of this intersegment regulatory network is essential for understanding the evolution of HA and NA and for improving sequence-based predictions regarding their function.

The decreased viral replication in guinea pigs infected with either of two *cis*-acting NA mutants (NA:K239R and NA:G339S) highlights the importance of HA/NA functional balance in viral fitness. It further shows that the increased fitness associated with NP:F346S cannot be explained by simple reduction in per-virion NA activity. Instead, these results raise several other nonmutually exclusive possibilities: (*i*) Other independent effects of the NP:F346S mutation are sufficiently beneficial to outweigh the detrimental effect of reduced NA expression; (*ii*) reduced NA activity can be advantageous, but only when combined with other effects of the NP:F346S mutation (i.e., increased SI particle production); (*iii*) NP:F346S reduces NA on virions in a way that is qualitatively distinct from the NA mutations tested here (e.g., the spatial distribution of NA on the particle surface) and thus has a different effect on host interactions; (*iv*) selective reduction in NA RNA synthesis, rather than NA content in virions, is critical to the NP:F346S phenotype in guinea pigs.

Regardless of the answer(s), these results highlight the dangers of oversimplification when attempting to attribute a fitness benefit to a given set of measured parameters.

The observation that IAV can selectively reduce the relative packaging frequency of individual gene segments undermines the dogma that IAV genome segments are copackaged in equimolar ratios with high efficiency (9–11). Instead, packaging efficiency is clearly variable and can be modulated rapidly (via a single-nucleotide substitution) in response to selective pressure. Importantly, decreased gene-packaging frequency can be associated with enhanced in vivo fitness, likely because frequent coinfection and complementation allow particles with incomplete genome sets to contribute to the propagation of the population. Under these conditions, the costs of producing SI particles may be outweighed by the potential benefits, the most important of which might be promoting reassortment and thus the adaptive potential of the population (4, 7).

If controlling the efficiency of gene-segment packaging is a common feature of IAV biology, different IAV strains should vary in the frequency with which different gene products are expressed within populations. Indeed, a panel of classic H1N1 viruses (all presumably egg-adapted) exhibited substantial differences in the frequencies of HA and NA, but not NP, expression that were stable across three passages in eggs (Fig. S7). These data indicate that variation in SI particle production, and potentially in gene-packaging efficiency, is widespread among IAV strains. As a practical matter, these findings also highlight the shortcomings of propagation-based infectivity assays (including plaque assays and infectious endpoint assays), which fail to measure SI particles, the predominant output of IAV infection (13). Efforts to compare infectivity between different strains or mutants may need to account for differences in SI particle production.

We have demonstrated that IAV consists of a minor fraction of fully infectious virions supported by a larger pool of SI particles that collectively influence the behavior of the population and whose abundance can be genetically controlled. Thus, the

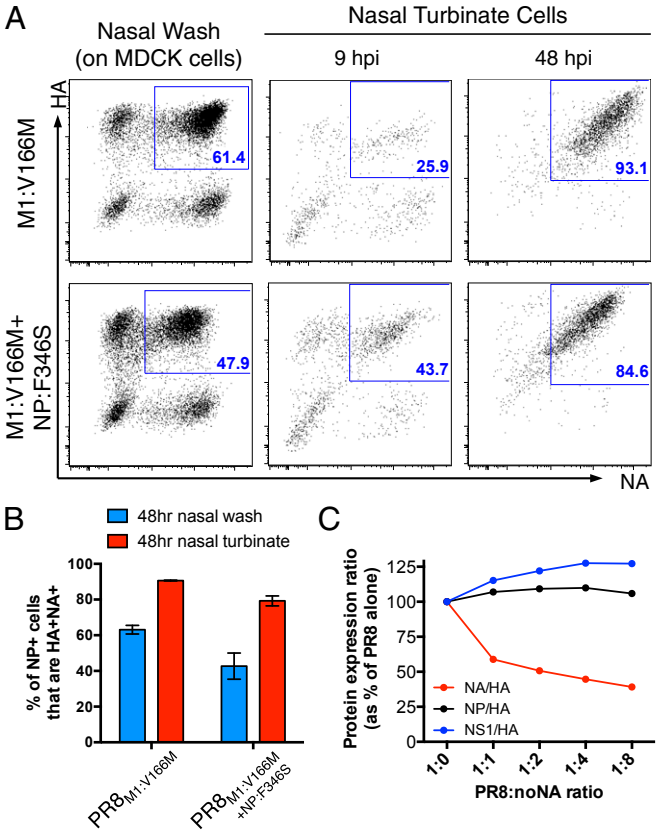

Fig. 6. Coinfection is common in the guinea pig upper airway during IAV infection. (*A* and *B*) Guinea pigs were infected i.n. with 10^3 $TCID_{50}$ (or 10^6 for the 9 hpi time point) of $PR8_{M1:V166M}$ or $PR8_{M1:V166M+NP:F346S}$. Nasal wash and turbinates were collected 9 and 48 hpi. (*A*) Representative dot plots showing NP^+ MDCK cells following ex vivo infection at an MOI <0.05 with 48 hpi nasal wash or NP^+ nasal turbinate cells collected at 9 or 48 hpi. (*B*) The percentage of 48 hpi NP^+ nasal turbinate cells that also were HA^+NA^+ was determined and compared with MDCK cells infected at an MOI <0.05 with nasal washes from the same animals. Data represent the mean ± SD of two animals per virus. (*C*) Relative expression of HA, NP, NA, and NS1, as determined by flow cytometry, in $HA^+NP^+NA^+$ Vero cells following infection with $PR8_{WT}$ at an MOI of 10 HAEU per cell alone or with increasing doses of $PR8_{NoNA}$. Data represent the mean percentage change in ratios of the indicated proteins compared with $PR8_{WT}$ alone ± SEM for three technical replicates.

complexity of IAV populations extends beyond the classical quasispecies description, and efforts to understand IAV infections also must account for relative gene-segment frequencies in viral populations. Further, our results reveal a possible role for SI particles and incomplete gene-segment packaging in determining viral fitness and transmissibility during species adaptation. In turning a seeming liability into in an asset, IAV once again demonstrates the amazing cleverness of viruses, which, with such a limited genetic palate, must exploit every possible trick for maximizing transmission.

Materials and Methods

Animal Care. All animal procedures were carried out in compliance with the Public Health Service policy, Office of Laboratory Animal Welfare guidance, and all guidelines of the National Institute of Allergy and Infectious Diseases (NIAID) Institutional Animal Care and Use Committee (IACUC). Research was conducted under a protocol approved by the NIAID IACUC.

Viruses. The A/Puerto Rico/8/1934 (PR8) strain was generated using an eight-plasmid rescue system (35) (GenBank accession nos. AF389115–AF389122), generously contributed by Adolfo Garcia-Sastre (Mt. Sinai School of Medicine, New York). These clones differ from the published sequence (above) at two positions: PB1 A549C (K175N) and HA A651C (I207L) (H1 numbering). We generated seed virus by transfecting 293T cells with the appropriate eight plasmids. Output virus then was expanded once in MDCK cells. Molecular clone-derived mutants were generated using site-directed mutagenesis as described previously (36). Molecular clone-derived viruses were expanded either on MDCK cells in Gibco minimal essential medium with GlutaMAX (Life Technologies) supplemented with 1 μg/mL trypsin treated with L-(tosylamido-2-phenyl) ethyl chloromethyl ketone (TPCK-treated trypsin) or within 10-d-old specific pathogen-free (SPF) embryonated chicken eggs. All tissue-culture virus titers were determined by end-point dilution on MDCK cells, and the $TCID_{50}$ was determined using the Reed–Muench method. Physical virus particles were enumerated using turkey RBCs as previously described (37), based on the observation that at hemagglutination end point the number of particles equals the number of erythrocytes. Titers of HA-expressing units (HAEU) and NA-expressing units (NAEU) were determined by infecting cultures of MDCK cells with serial dilutions of virus. After 16 h in the presence of neutralizing mAb H17-L2, the percentages of cells expressing HA and/or NA were detected by flow cytometry and then were combined with cell counts to calculate the concentration of virions capable of HA or NA expression. Seven-segment viruses ($PR8_{NoNA}$) were generated via the eight-plasmid method described above, omitting the plasmid encoding genome segment 6. After transfection, $PR8_{NoNA}$ viruses were harvested and propagated in MDCK cells by sequential overnight infections followed by release by treatment with cholera filtrate (Sigma). The H1N1 strains A/SW/31, A/New Jersey/76, A/Texas/36/91, A/Fort Monmouth/1/47, A/Denver/57, A/Weiss/43, and A/Malaysia/54 were maintained by low-MOI passage in 10-d-old SPF embryonated chicken eggs.

Additional information on materials and methods can be found in *SI Materials and Methods*.

ACKNOWLEDGMENTS. This work was funded by the Division of Intramural Research, National Institutes of Allergy and Infectious Diseases, National Institutes of Health.

1. Molinari NA, et al. (2007) The annual impact of seasonal influenza in the US: Measuring disease burden and costs. *Vaccine* 25(27):5086–5096.
2. Nelson MI, et al. (2008) Multiple reassortment events in the evolutionary history of H1N1 influenza A virus since 1918. *PLoS Pathog* 4(2):e1000012.
3. Holmes EC, et al. (2005) Whole-genome analysis of human influenza A virus reveals multiple persistent lineages and reassortment among recent H3N2 viruses. *PLoS Biol* 3(9):e300.
4. Ince WL, Gueye-Mbaye A, Bennink JR, Yewdell JW (2013) Reassortment complements spontaneous mutation in influenza A virus NP and M1 genes to accelerate adaptation to a new host. *J Virol* 87(8):4330–4338.
5. Bonhoeffer S, Chappey C, Parkin NT, Whitcomb JM, Petropoulos CJ (2004) Evidence for positive epistasis in HIV-1. *Science* 306(5701):1547–1550.
6. Kondrashov AS (1988) Deleterious mutations and the evolution of sexual reproduction. *Nature* 336(6198):435–440.
7. Keightley PD, Otto SP (2006) Interference among deleterious mutations favours sex and recombination in finite populations. *Nature* 443(7107):89–92.
8. Hutchinson EC, von Kirchbach JC, Gog JR, Digard P (2010) Genome packaging in influenza A virus. *J Gen Virol* 91(Pt 2):313–328.
9. Chou YY, et al. (2012) One influenza virus particle packages eight unique viral RNAs as shown by FISH analysis. *Proc Natl Acad Sci USA* 109(23):9101–9106.
10. Noda T, et al. (2006) Architecture of ribonucleoprotein complexes in influenza A virus particles. *Nature* 439(7075):490–492.
11. Noda T, et al. (2012) Three-dimensional analysis of ribonucleoprotein complexes in influenza A virus. *Nat Commun* 3:639.
12. McGeoch D, Fellner P, Newton C (1976) Influenza virus genome consists of eight distinct RNA species. *Proc Natl Acad Sci USA* 73(9):3045–3049.
13. Brooke CB, et al. (2013) Most influenza a virions fail to express at least one essential viral protein. *J Virol* 87(6):3155–3162.
14. Brooke CB (2014) Biological activities of 'noninfectious' influenza A virus particles. *Future Virol* 9:41–51.
15. Palese P, Tobita K, Ueda M, Compans RW (1974) Characterization of temperature sensitive influenza virus mutants defective in neuraminidase. *Virology* 61(2):397–410.
16. Liu C, Eichelberger MC, Compans RW, Air GM (1995) Influenza type A virus neuraminidase does not play a role in viral entry, replication, assembly, or budding. *J Virol* 69(2):1099–1106.
17. Job ER, et al. (2014) A single amino acid substitution in the hemagglutinin of H3N2 subtype influenza A viruses is associated with resistance to the long pentraxin PTX3 and enhanced virulence in mice. *J Immunol* 192(1):271–281.
18. Matrosovich MN, Matrosovich TY, Gray T, Roberts NA, Klenk HD (2004) Neuraminidase is important for the initiation of influenza virus infection in human airway epithelium. *J Virol* 78(22):12665–12667.
19. Wagner R, Matrosovich M, Klenk HD (2002) Functional balance between haemagglutinin and neuraminidase in influenza virus infections. *Rev Med Virol* 12(3):159–166.
20. Yen HL, et al. (2011) Hemagglutinin-neuraminidase balance confers respiratory-droplet transmissibility of the pandemic H1N1 influenza virus in ferrets. *Proc Natl Acad Sci USA* 108(34):14264–14269.
21. Xu R, et al. (2012) Functional balance of the hemagglutinin and neuraminidase activities accompanies the emergence of the 2009 H1N1 influenza pandemic. *J Virol* 86(17):9221–9232.
22. Hensley SE, et al. (2011) Influenza A virus hemagglutinin antibody escape promotes neuraminidase antigenic variation and drug resistance. *PLoS ONE* 6(2):e15190.
23. Das SR, et al. (2013) Defining influenza A virus hemagglutinin antigenic drift by sequential monoclonal antibody selection. *Cell Host Microbe* 13(3):314–323.
24. Hirst GK, Pons MW (1973) Mechanism of influenza recombination. II. Virus aggregation and its effect on plaque formation by so-called noninfective virus. *Virology* 56(2):620–631.
25. Barry RD (1961) The multiplication of influenza virus. II. Multiplicity reactivation of ultraviolet irradiated virus. *Virology* 14:398–405.
26. Marshall N, Priyamvada L, Ende Z, Steel J, Lowen AC (2013) Influenza virus reassortment occurs with high frequency in the absence of segment mismatch. *PLoS Pathog* 9(6):e1003421.
27. Tao H, Steel J, Lowen AC (2014) Intrahost dynamics of influenza virus reassortment. *J Virol* 88(13):7485–7492.
28. White DO, Cheyne IM (1966) Early events in the eclipse phase of influenza and parainfluenza virus infection. *Virology* 29(1):49–59.
29. Ilyushina NA, Bovin NV, Webster RG (2012) Decreased neuraminidase activity is important for the adaptation of H5N1 influenza virus to human airway epithelium. *J Virol* 86(9):4724–4733.
30. Bloom JD, Gong LI, Baltimore D (2010) Permissive secondary mutations enable the evolution of influenza oseltamivir resistance. *Science* 328(5983):1272–1275.
31. Matsuoka Y, et al. (2009) Neuraminidase stalk length and additional glycosylation of the hemagglutinin influence the virulence of influenza H5N1 viruses for mice. *J Virol* 83(9):4704–4708.
32. Shtyrya Y, et al. (2009) Adjustment of receptor-binding and neuraminidase substrate specificities in avian-human reassortant influenza viruses. *Glycoconj J* 26(1):99–109.
33. Campbell PJ, et al. (2014) The M segment of the 2009 pandemic influenza virus confers increased neuraminidase activity, filamentous morphology, and efficient contact transmissibility to A/Puerto Rico/8/1934-based reassortant viruses. *J Virol* 88(7):3802–3814.
34. Moulès V, et al. (2011) Importance of viral genomic composition in modulating glycoprotein content on the surface of influenza virus particles. *Virology* 414(1):51–62.
35. Martínez-Sobrido L, García-Sastre A (2010) Generation of recombinant influenza virus from plasmid DNA. *J Vis Exp* (42):e2057.
36. Vallejo AN, Pogulis RJ, Pease LR (2008) PCR mutagenesis by overlap extension and gene SOE. *Cold Spring Harb Protoc*, 10.1101/pdb.prot4861.
37. Donald HB, Isaacs A (1954) Counts of influenza virus particles. *J Gen Microbiol* 10(3):457–464.